Geophys. J. Int. (2008) doi: 10.1111/j.1365-246X.2008.04020.x

Site effect evaluation in the basin of Santiago de Chile using ambient noise measurements

Sylvette Bonnefoy-Claudet,[1]* Stéphane Baize,[1] Luis Fabian Bonilla,[1] Catherine Berge-Thierry,[1] Cesar Pasten,[2] Jaime Campos,[3] Philippe Volant[1] and Ramon Verdugo[2]

[1]*Institute for Nuclear Safety and Radioprotection, Fontenay-aux-Roses, France*
[2]*Department of Civil Engineering, University of Chile, Chile*
[3]*Department of Geophysics, University of Chile, Chile*

Accepted 2008 October 24. Received 2008 October 24; in original form 2007 November 28

SUMMARY

We performed extensive ambient vibration measurements in the basin of Santiago de Chile (Chile), and we look for testing the reliability of the horizontal-to-vertical amplitude spectra ratio method (*H/V*) as a tool to provide qualitative and quantitative information of site effects in complex geological media. The interpretation of the *H/V* data was carried out conformably to the SESAME project consensus criteria and outlines three major patterns: (1) clear peaked *H/V* curves related to sharp underground velocity contrast; (2) *H/V* peak of low amplitude and flat curve related to weak contrast and (3) broad *H/V* peak indicating the presence of strong lateral variations of underground structure. *H/V* measurements, however, reveal a discrepancy between the computed soil resonance frequencies and the expected building resonance, therefore not leading to a straight interpretation of the intensity distribution derived from observed damage to one storey houses in Santiago after the 1985 Valparaiso earthquake. Indeed, the *H/V* technique mostly maps the first fundamental frequency; however, it fails to show higher resonance modes. In the case of the city of Santiago, this method works well for assessing the seismic hazard for high-rise buildings, but is questionable for smaller structures as is the case of a great percentage of constructions in the city.

Key words: Site effects; South America.

1 INTRODUCTION

Chile is one of the most seismic areas in the world. Before the great Sumatra–Andaman earthquake (2004, $M_w = 9.1$, Lay *et al.* 2005), 46 per cent of the seismic energy spread out during the last century was in Chile. The largest events that occurred in Chile (e.g. 1960 Valdivia, $M_w = 9.5$, 1985 Valparaiso, $M_w = 8$, and 1995 Antofagasta, $M_w = 8.1$) are mostly due to the subduction of the Nazca Plate beneath the South American Plate (Pardo *et al*. 2002; Barrientos *et al.* 2004; Gardi *et al.* 2006). In central Chile, the subduction raises a relative velocity of about 8 cm yr^{-1} in a N78°E direction (De Mets *et al.* 1994) and generates mostly interplate earthquakes. The recurrence of the largest events in the Metropolitan region—Santiago de Chile area—is about 80 yr.

When an earthquake occurs, the most likely factor that contributes to damages and human injuries is the proximity of the hypocentre to populated areas. However, ground amplification effect can become predominant at far distances due to the local geology. The Michoacan earthquake (Mexico, 1985, $M_w = 8.1$) and the Great Hanshin-Awaji earthquake (1995 Kobe, $M_w = 6.9$) are outstanding examples of such site effects. In Chile, most of the seismological studies focus on the properties of the subduction processes; however, a recent study has shown that local site effects may happen in Santiago de Chile (Cruz *et al.* 1993).

It was the Valparaiso earthquake in 1985 that showed that the town of Santiago, Chile's capital city (five million inhabitants), was prone to site effects (Monge 1986). The seismic intensities (MSK) derived from observed damages to one storey adobe and one storey un-reinforced masonry houses during the 1985 earthquake were locally much higher (up to IX) than expected (VI) according to regional attenuation relations (Astroza & Monge 1987; Astroza *et al.* 1993). The highest intensities were mainly reported in areas with poor soils conditions, in the fine-grained alluvial deposit and in the ashes deposits (Astroza & Monge 1991). Local site effects due to "superficial" geological conditions were first suspected to happen in which was previously thought to be a good foundation soil. Despite this 'first-order' correlation between superficial geology and damage, some discrepancies are notable: some parts of the most damaged areas are not built on soft sediments, and some soft sediment areas did not show strong damage (Fernandez Mariscal 2003).

*Now at: Résonance Ingénieurs-Conseils SA, 21 rue Jacques Grosselin, 1227 Carouge (GE), Switzerland. E-mail: sylvette.bonnefoy-claudet@resonance.ch

Thus, the geometry of the basin and the geology of deep sediments were suspected to be partly responsible for these amplified effects. Such 2-D or 3-D basin structural effects on wave propagation have been illustrated for long time through observational (Uetake & Kudo 1998) and numerical studies (Kawase 1996; Olsen & Archuleta 1996).

Past investigations were conducted in Santiago de Chile to evaluate site effects. An array of accelerometers (SMACH array) has been deployed since 1989 and local site effects have been evaluated from strong ground motion records (Midorikawa *et al.* 1991; Cruz *et al.* 1993). Ambient vibrations measurements were also carried out in the city to correlate the site effects evaluated by strong ground motion (Guéguen 1994; Toshinawa *et al.* 1996). Ambient vibration studies such as the *H/V* technique (Nakamura 1989) are powerful tools to study local soil site effects. In addition to mapping the resonance frequencies of the soil, the *H/V* technique has been used in recent studies as an alternative tool to classical geophysical exploration for characterizing sediment infilling—typically, the sediment thickness or average shear velocity—by taking advantage of the simple relation ($F_0 = \beta/4h$) between the resonance frequency (f_0), the average shear wave velocity (β) and the average sediment thickness (h) (Ibs-Von Seht & Wolhenberg 1999; Delgado *et al.* 2000; Parolai *et al.* 2002). Although reliable in horizontal layering (Bonnefoy-Claudet *et al.* 2006a), this simple interpretation—that assumes 1-D wave propagation—may be misleading in case of 2-D or 3-D structures. Such examples have been shown not only experimentally (Uebayashi 2003; Gueguen *et al.* 2007) but also numerically (Guillier *et al.* 2006). This discrepancy is mainly due to the complexity of surface wave propagation in 2-D/3-D structures. When the basement geometry is far from 1-D structure, the propagation of seismic waves (body and surface waves) may involve diffracted surface waves generated along slopes and discontinuities. In such situation, the diffracted surface waves, in addition to 1-D resonance effect, may be responsible for site amplification of seismic ground motion. The contamination of ambient noise wavefield by edge-diffracted waves has been already outlined in previous studies (Cornou 2002; Di Giulio *et al.* 2006).

The scope of this work is to verify the limitation of the *H/V* technique as a tool to provide qualitative and quantitative information of site conditions when investigating 3-D structures. The study was carried out in Santiago de Chile basin, which is known to be affected by 3-D geometrical and geological features.

2 GEOLOGICAL SETTING

The city of Santiago de Chile is located in the so-called Central Depression, which is a basin surrounded by the Main and Coastal ranges of the Andes (western 70° and southern 33°). This basin spans 80 km long and 30 km wide, and it is mainly elongated in the north–south direction. The basin is characterized by the coalescence of three main alluvial cones that drain the Andean Cordillera: cones of Colina, Mapocho and Maipo (Fig. 1).

Due to the geomorphological setting, the basin is essentially filled with alluvial sediments (Valenzuela 1978). These sediments have extensively been characterized when looking for water and construction material resources (Falcon Moreno *et al.* 1970; Morales-Jerez 2002). They are composed of pebbles, gravels, clays and volcanic ashes (Fig. 2). The pebbles and gravels are mainly located in the eastern and southern part of the basin. Clayey material is mostly present in the north; whereas a transition zone is found in the centre

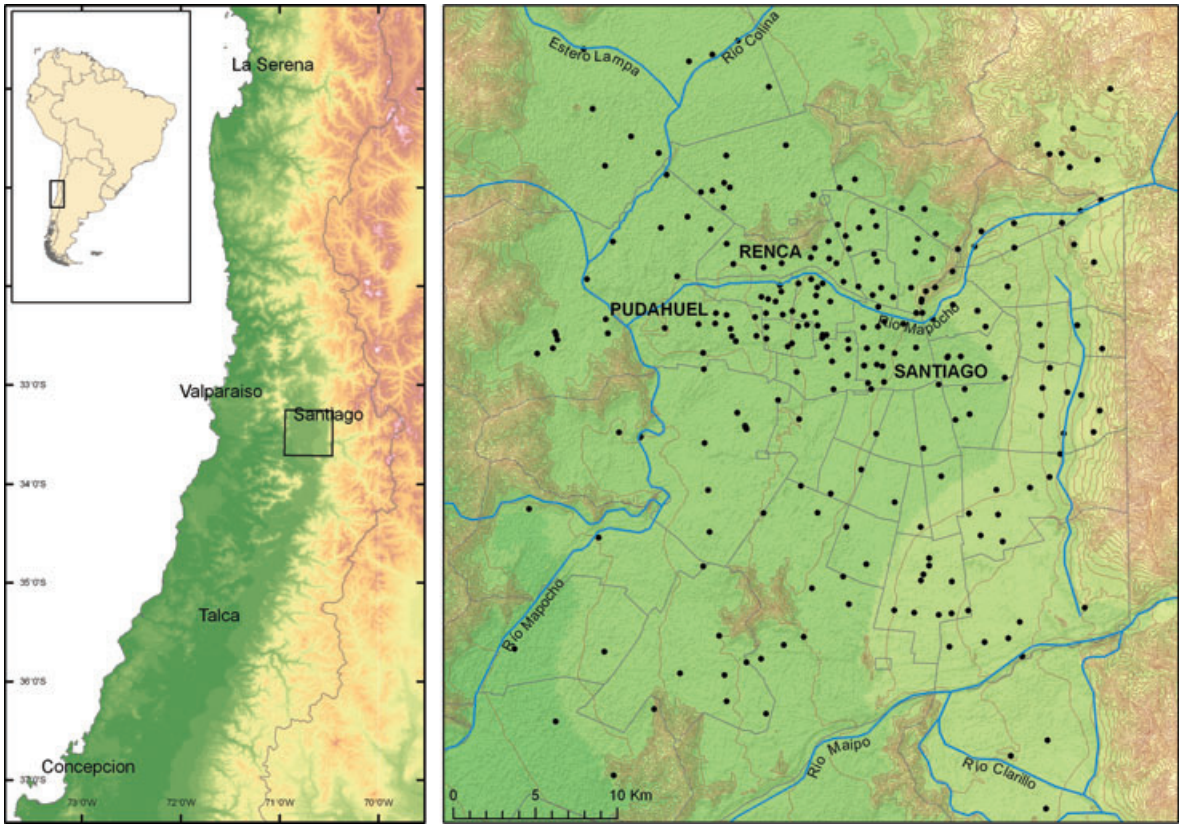

Figure 1. Left-hand panel: location of the Santiago de Chile basin (Chile). Right-hand panel: spatial distribution of the *H/V* measurement points in the basin (black dots). Black lines show Santiago districts. Background colour displays the digital elevation model and brown lines indicate the elevation contour lines. Blue lines exhibit major rivers.

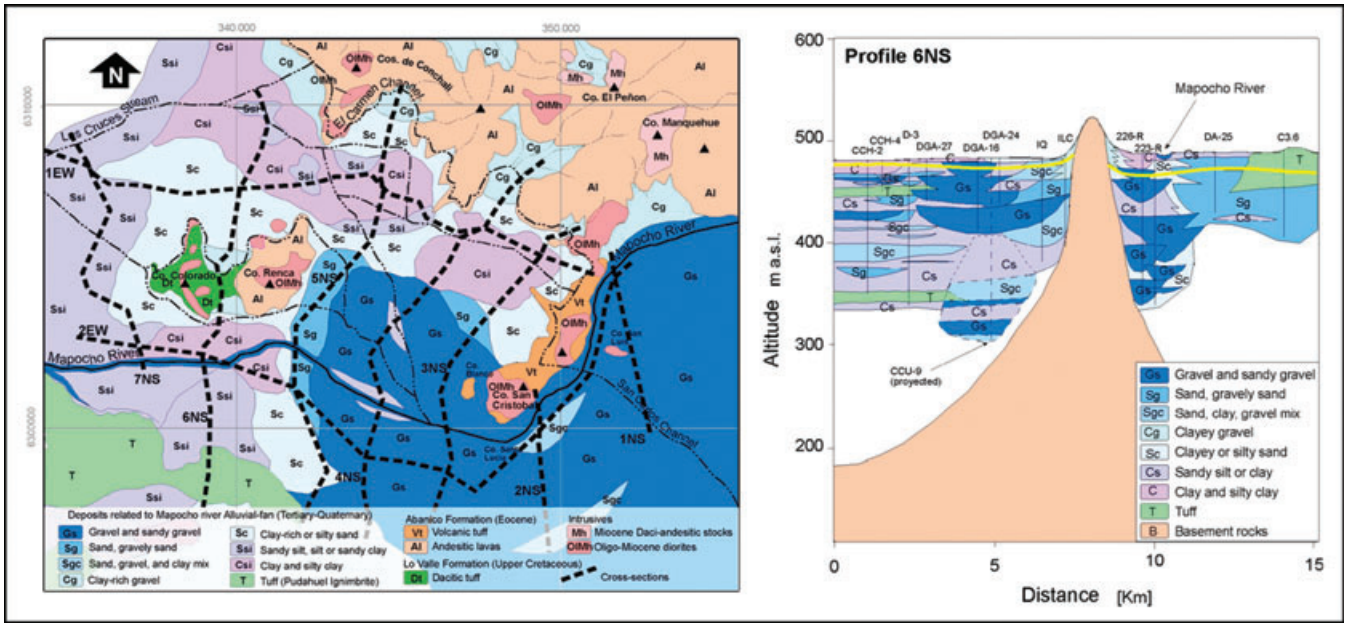

Figure 2. Left-hand panel: map of geological cross-sections in the North Western part of Santiago de Chile. Right-hand panel: Geological cross-section along profile 6NS. After Iriarte-Diaz (2003).

Table 1. Mechanical properties (*P*- and *S*-waves velocity, density) at various depths of the three main formations observed in the basin of Santiago (gravels, clays and ashes; after Bravo 1992; Guéguen 1994).

	Depth (m)	V_P (m s^{-1})	V_S (m s^{-1})	Density (g cm^{-3})
Gravels	0–20	950–1250	480–720	2–2.3
	200		1300	2.1
	500		2000	2.1
Clays	0–20	400–1000	120–350	1.2–1.8
	50		550	2.1
	500		2000	2.1
Ashes	0–20	400–900	180–450	1.15–1.7

of the valley. In the Pudahuel district, a 40-m-thick layer of ashes (Pudahuel ignimbrite, also known as pumices) is known to seat at the top of the sedimentary column. The stiff pumice probably comes from a major eruption of the Maipo volcano, located at around 120 km to the southeast, at the head of the Maipo valley.

The geometry and depth of the basement geometry are constrained by gravimetric data (Araneda *et al.* 2000), geophysical surveys (Bravo 1992) and borehole data (Iriarte-Diaz 2003; Morales-Jerez 2002). These data were used to construct a first-order geological model of the basin (Baize *et al.* 2006). Although the spatial extension of each formation at depth is not well constrained; most of the studies depict a complexity of the basin geometry, outlining very sharp lateral and vertical variations of units.

In addition, the estimation of *P*- and *S*-wave velocities of the three main formations (stiff sediments, unconsolidated sediments and pumice) are inferred from seismic refraction (Bravo 1992; Guéguen 1994) and summarized in Table 1. The shear wave velocity in the rock substratum is about 2000 m s^{-1} (Bravo 1992).

3 *H/V* AMBIENT VIBRATIONS DATA

Extensive ambient noise measurements were performed in the basin of Santiago from April 2005 to Spring 2007. The ambient noise vibrations were recorded using Cityshark I and Cityshark II data loggers coupled to sensors Lennartz LE-3-D (three components velocimeters having a 5 s natural period). 264 measurements of ambient noise were collected in the city (Fig. 1). The sampling rate was 125 Hz and the duration of recording 15 min, except at some points where the recording duration was extended to 20 minutes because of a strongly disturbed environment (dense and close car traffic, pedestrians, etc.). Some signals, however, were still dominated by transients, thus 37 records were rejected. Finally, 227 measurements of ambient noise were considered for the *H/V* processing.

The microtremor *H/V* technique was first proposed by Nogoshi & Igarashi (1971) and widespread by Nakamura (1989). It consists in estimating the ratio between the Fourier amplitude spectra of the horizontal and the vertical components of ambient noise vibrations. In this study, *H/V* ratios are calculated using the GEOPSY software (http://www.geopsy.org). *H/V* ratios are calculated for the frequency range 0.2–10 Hz, using 50 s time windows and removing time windows contaminated by transients. The objective is to assure the stationary of ambient vibrations, and to avoid the transients often associated with specific urban sources (footsteps, close traffic). The procedure to detect transients is based on a classical comparison between the short term average (‘*STA*’, the average level of signal amplitude over a short period of time, 1 s) and the long term average ‘*LTA*’ (the average level of signal over a much longer period of time, 30 s). Only windows with *STA*/*LTA* ratio between 0.3 and 2 are kept for the *H/V* computation. For every selected time window, the Fourier amplitude spectra are smoothed with a Konno & Ohmachi (1998) filter using a coefficient of 40 for the bandwidth. The quadratic mean of the horizontal amplitude spectra is used here. The final *H/V* ratio and the associated standard deviation are obtained by averaging the *H/V* ratios from all windows. The standard deviations on *H/V* ratio curves are estimated considering the arithmetic average for all individual logarithm of *H/V* ratio computed for each time window. See Atakan *et al.* (2004) for further details.

The field experiment and the parameters of calculation followed the recommendations of the SESAME consortium (Bard & SESAME-Team 2005) to verify the reliability of results:

(1) The length of time windows (*Lw*) should be larger to 10 times the period of interest (i.e. the period corresponding to the *H/V* ratio peak frequency *Fhv*): $Lw > 10 \times Fhv$.

(2) It is recommended to compute *H/V* ratio over a sufficient number of windows to assess the average *H/V* curve. The number of windows (*Nw*) should be set up according to *H/V* peak frequency and windows length: $Lw \times Nw \times Fhv > 200$, the value 200 was arbitrarily chosen by the SESAME consortium.

(3) An acceptably low level of scattering between all windows is needed. The standard deviation of the mean *H/V* curve should thus remain low over a frequency range at least equal to ($0.5 \times Fhv$, $2 \times Fhv$). It is recommended that the standard deviation should be lower than a factor of two times (for $Fhv > 0.5$ Hz)—or a factor of three times (for $Fhv < 0.5$ Hz)—the mean *H/V* curve.

The average *H/V* curves were systematically analysed with respect to the processing parameters following the SESAME recommendations. At the end, 199 reliable *H/V* curves fulfilled these criteria; only these data will be considered in the next sections. Fig. 3 shows an example of ambient noise record and its associated *H/V* curve.

Among the 199 reliable *H/V* curves, 39 data exhibits *H/V* curves showing large standard deviation for frequencies below 1 Hz (Fig. 4a). The records corresponding to these data are widespread over the city of Santiago and do not show any spatial correlation. The very large amplitude of the standard deviation suggests that its origin is not linked to geological or geometrical effects. Such large standard deviation associated to a clear trend may be related to strong wind during the recording (Mucciarelli *et al.* 2005; Chatelain *et al*. 2008). However, in the case of Santiago, this hypothesis has to be discarded since there was no wind at all during the measurements. On the other hand, since the measurements were made in urban area and over great distances, a bad soil-sensor coupling may be responsible for the bad definition of these *H/V* curves. We tested this hypothesis by simultaneously recording ambient noise at four kinds of surfaces, which are representative of the soil coverage in Santiago: grassy ground and pavements with different sizes of paving stones. The sensors were placed at the soil surface over a short distance of about 5 m. The *H/V* curve recorded on the thin layer of grass is flat and shows low standard deviation (Fig. 4c), whereas the *H/V* curves recorded on pavements exhibit very large standard deviation for frequencies below 1 Hz (Fig. 4b shows a *H/V* curve observed at only one kind of pavement) and reproduce well the large uncertainties observed on actual *H/V* curve shown in Fig. 4(a). These observations strongly suggest that a poor soil-sensor coupling has a large influence on the shape of the *H/V* curve at low frequencies. Nevertheless, more systematic measurements should be carried out to provide a final explanation. Note that this strong disturbance does not influence the *H/V* curve for frequencies higher than 1 Hz.

4 DISTRIBUTION OF THE *H/V* CURVES

4.1 Topology of the *H/V* curves

Detailed analysis of the *H/V* data measured in Santiago indicates that the shape of the *H/V* curves is not uniform: 47 *H/V* curves (24 per cent of reliable data) do not show any peak (Fig. 5a), whereas 152 *H/V* curves (76 per cent of reliable data) show at least one peak. In total, we count 187 *H/V* peaks which can be separated in two groups: clear peaks and those with no easy peak identification. The criteria to qualify how neat a peak is are based on the amplitude of the *H/V* peak, its relative amplitude value with respect to other peaks in other frequency bands and the relative value of the standard deviation. We test the clarity of the *H/V* peaks in Santiago using the following recommendations proposed by SESAME guidelines (Bard & SESAME-Team 2005).

(1) The *H/V* peak amplitude (*Ahv*) should be higher than 2.

(2) There exists one frequency (f^-), lying between *Fhv*/4 and *Fhv*, such that $Ahv/A(f^-) > 2$, with $A(f^-)$ the *H/V* ratio amplitude at the frequency f^-.

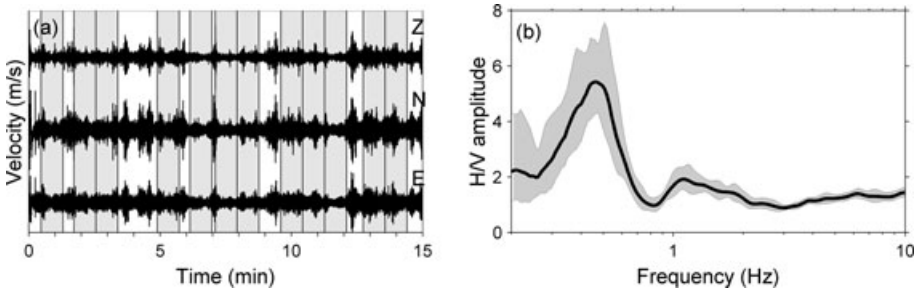

Figure 3. (a) Example of ambient seismic noise records: vertical (Z), north–south (N) and east–west (E) components. Greyed areas depict the time windows selected for the *H/V* ratio computation. (b) Corresponding *H/V* curve (black line) and the associated standard deviation (greyed surface).

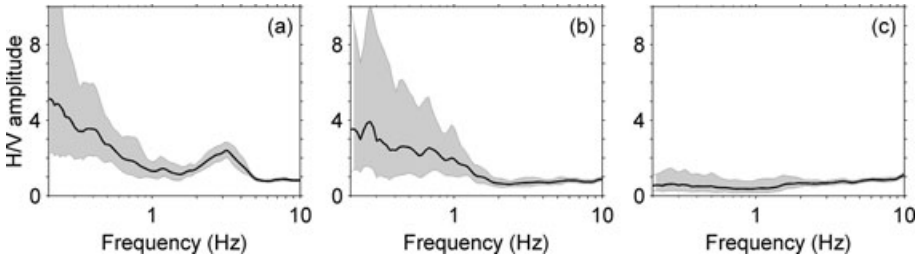

Figure 4. (a) Example of observed *H/V* curve showing a large standard deviation at low frequency. *H/V* ratios computed at two kind of soil: (b) one kind of pavement, which is typical of Santiago de Chile, and (c) on grass. The distance between the two former measurements was about 5 m, and the ambient noise was recorded simultaneously by two Lennartz 5 s. See the legend of *H/V* curve (Fig. 3).

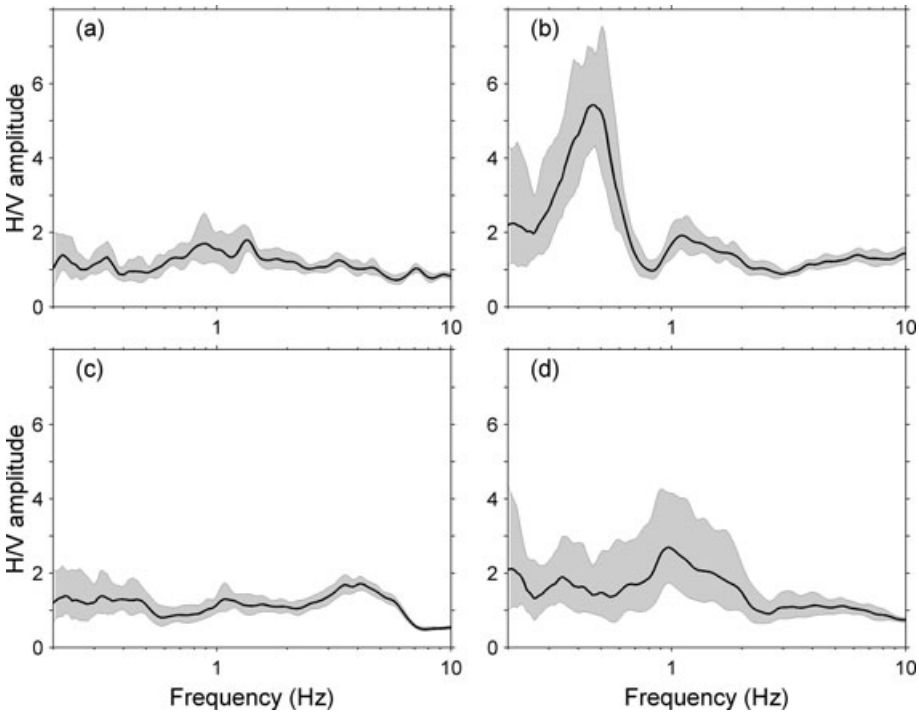

Figure 5. Topology of the *H/V* curves observed in Santiago de Chile area: (a) flat curves, (b) curves showing a clear peak, which satisfy the SESAME criteria, and curves showing unclear peaks which do not fully satisfy the SESAME criteria: peaks of low amplitude (c) and broad peaks (d).

(3) There exists one frequency (f^+), lying between *Fhv* and $4 \times$ *Fhv*, such that $Ahv/A(f^+) > 2$, with $A(f^+)$ the *H/V* ratio amplitude at the frequency f^+.

(4) The standard deviation should be lower than a frequency dependent threshold (see Bard & SESAME-Team 2005 for further details).

When the *H/V* peak fulfilled at least 3 among these 4 criteria, then there is quasi-certitude that the site under study presents a large velocity contrast at some depth and is very likely to amplify the ground motion. The *H/V* peak frequency *Fhv* can be considered as a very reliable estimate of the fundamental frequency. In the case of Santiago, 77 *H/V* peaks satisfy the clarity criteria. Fig. 5(b) displays an example of such clear peak. The *H/V* peaks (110 data) that failed to fulfil the clarity criteria could be divided into two groups: peaks with low amplitude (lower than 2) (Fig. 5c) and broad peaks (large amplitude over a broad frequency band; Fig. 5d).

4.2 Spatial distribution of the *H/V* curves

The records corresponding to the clear *H/V* peaks are in great majority located in the central and northern parts of the basin (black triangles in Fig. 6). They are distributed at the surface of soft sediments: unconsolidated alluvial deposits or stiff pumice deposits. The shear wave velocity at the surface of these units is low (smaller than 350 m s^{-1}, Table 1) compared with the velocity in the bedrock (about 2000 m s^{-1}). This suggests the existence of strong velocity contrast at depth between unconsolidated and consolidated underlying sediment. Clear *H/V* peaks in Santiago are thus most probably correlated with this sharp contrast (Bard 1998).

The flat *H/V* curves and the *H/V* curves with peaks of low amplitude are mainly located in the southern and eastern parts of the basin, at the surface of the Santiago and Mapocho gravels (black and grey circles, respectively, in Fig. 6). As shown in Section 2, these units are characterized by stiff sediments with a rather high *S*-wave velocity at depth (1350 m s^{-1}; Table 1). The absence of neat peak on *H/V* curve in this area is thus very likely due to the local underground structure, which may not exhibit any sharp velocity contrast at any depth leading to low-to-moderate amplifications. The correlation between the absence of peak on *H/V* curve and weak velocity contrast has been already stressed in previous experimental and numerical studies (Konno & Ohmachi 1998; Bonnefoy-Claudet *et al.* 2008).

The broad *H/V* peaks (grey squares in Fig. 6) are in great majority located next to topographic slopes and deep depressions. There is also a swarm of broad peaks between Renca foothill and Pudahuel depression (in the centre of the basin). In addition to the broad peaks, the other types of *H/V* data are also present in this area. In this region, the rock basement rises to the surface at the Renca hill (350 m above free surface) and reaches 500 m deep below the surface 5000 m away (in Pudahuel depression; see Figs 2 and 7). The large variability of *H/V* data is thus most probably related to a complexity of the ambient noise wavefield, which may be diffracted along sloping bedrock–soft sediment contacts or some sloping internal stratification in the sedimentary cover, both cases having a high velocity contrast. Evidence of such effects has already experimentally been observed in Colfiorito basin, Italy, (Rovelli *et al.* 2001) and in Dinar basin, Turkey, (Yalcinkaya & Alptekin 2005) for instance.

To determine the origin of the broad peaks, we performed *H/V* measurements in the centre of the basin, along a profile from the Renca foothill (point P01) up to the trough of Pudahuel district (450 m deep; point P10). Ten measurements were done over a distance of 4500 m (see location of the profile in Fig. 6, red line). Points P01–P09 are located on unconsolidated sediments (silts and clays); point P10 is located on stiff pumice (Fig. 7). The duration of recording is 20 min and the *H/V* ratios are computed as described in Section 3. Fig. 8 shows spectrogram depicting the relationships

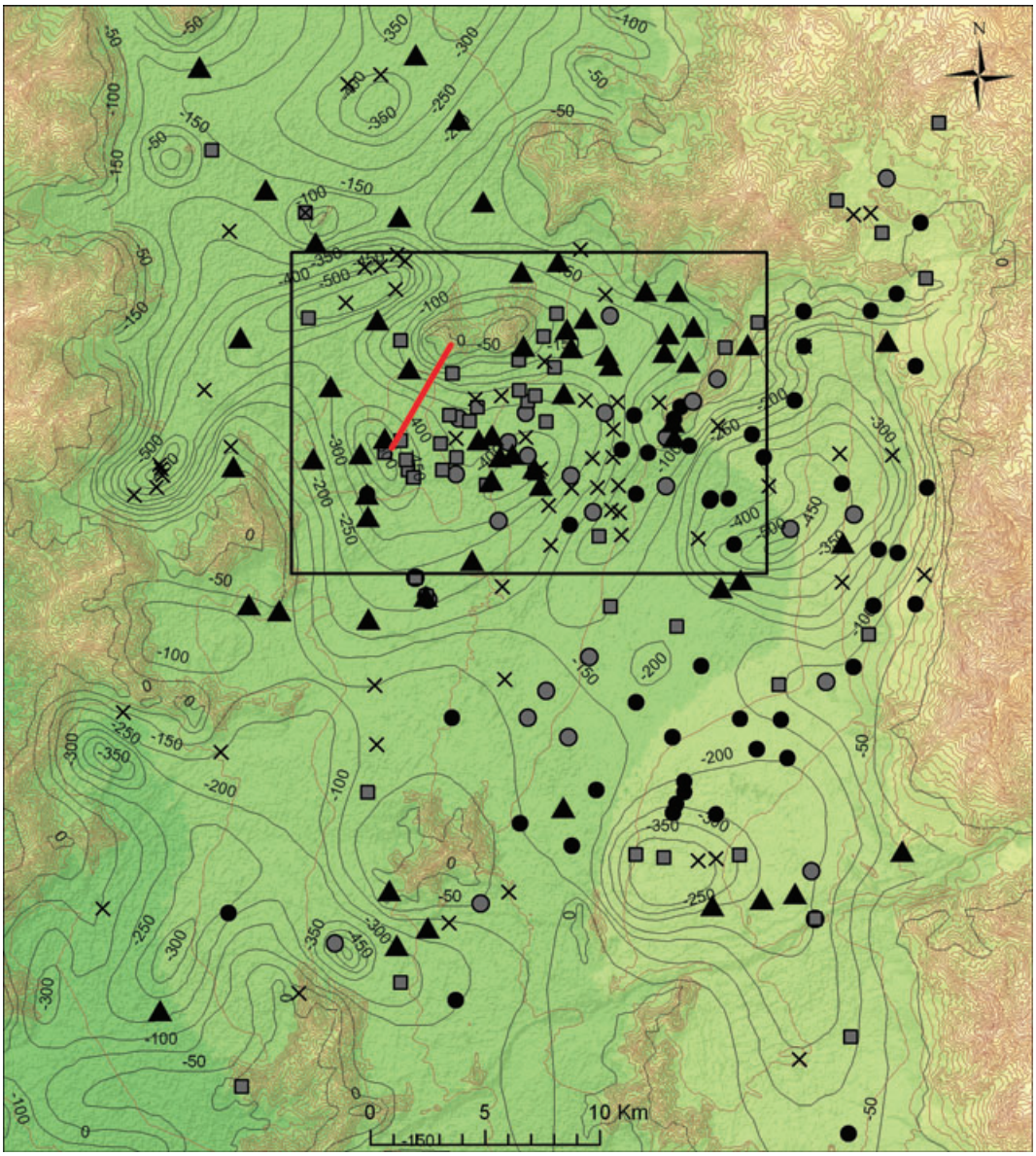

Figure 6. Spatial distribution of the various types of *H/V* data observed in Santiago: clear peaks (black triangles), peaks of low amplitude (grey circles), flat curves (black circles) and broad peaks (grey squares). Crosses indicate the location of rejected ambient noise records and no reliable *H/V* data. See Fig. 5 for an illustration of the *H/V* peak types. The black rectangle displays the location of map shown in Fig. 7. Red line indicates the position of the *H/V* profile.

between the *H/V* spectral ratio amplitude and location along the profile. The *H/V* peak frequency sharply decreases from point P01 ($Fhv = 3.5$ Hz) to P03 ($Fhv = 0.4$ Hz), then it steadily decreases up to point P10 ($Fhv = 0.35$ Hz). In addition, point P03 shows a second peak having a smaller amplitude at 1 Hz and points P05–P10 show a small bump between 1.5 and 2 Hz. Regarding the shape of the *H/V* curve, point P01 and points P04 to P10 show clear peaks (at least for the main peak), whereas *H/V* peaks associated to points P02 and P03 are much broader with lower amplitude. Because all the data are located at the surface of fine-grained soils (except P10 located on ashes), we assume that the discrepancy in *H/V* peak shape might not be related to the geology. On the other hand, gravimetric data (Araneda *et al.* 2000) shows that points P02 and P03 are located in the most rapidly varying thickness part of the profile; whereas the points P04–P10 are located in a gentler slope. Recent experimental studies (Woolery & Street 2002; Uebayashi 2003) and numerical studies (Uebayashi 2003; Guillier *et al.* 2006) have already portrayed the influence of steep slope on the shape of *H/V* curve. The irregular shape of the basement can lead to focusing or de-amplification and a loss of spatial coherency in the ambient noise motion at the surface (Woolery & Street 2002; Cornou *et al.* 2003). Taking into account the steep slope of the basement, the peculiar shapes of *H/V* curves (broad-bandwidth peaks) might be probably related to the more complex wavefield (diffracted body and surface waves) generated near the edge of the basement slope.

5 IMPLICATIONS FOR SITE EFFECTS ASSESSMENT

Most examples reported in the literature indicate clear peaked *H/V* curve for soft soils and almost flat curves for rock sites (Lermo & Chavez-Garcia 1994; Fäh 1997; Bour *et al.* 1998; Duval *et al.* 1994). Of course the amplitude and the frequency of the peak vary

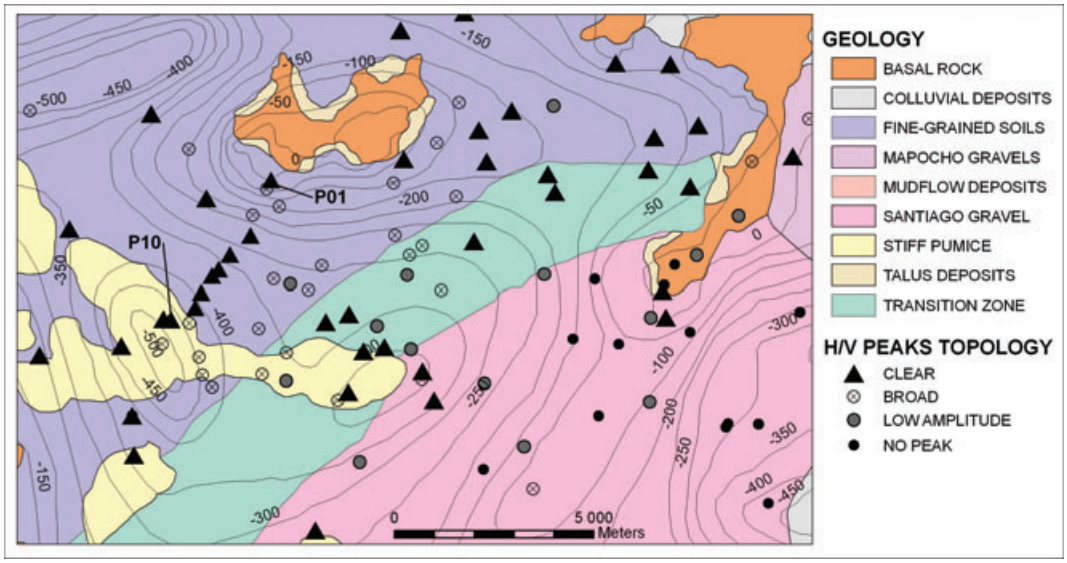

Figure 7. Spatial distribution of the various types of curve *H/V* in the centre of the basin of Santiago. See Fig. 6 for the spatial location of the map. The colour background shows the surface geology of the basin (after Valenzuela 1978).

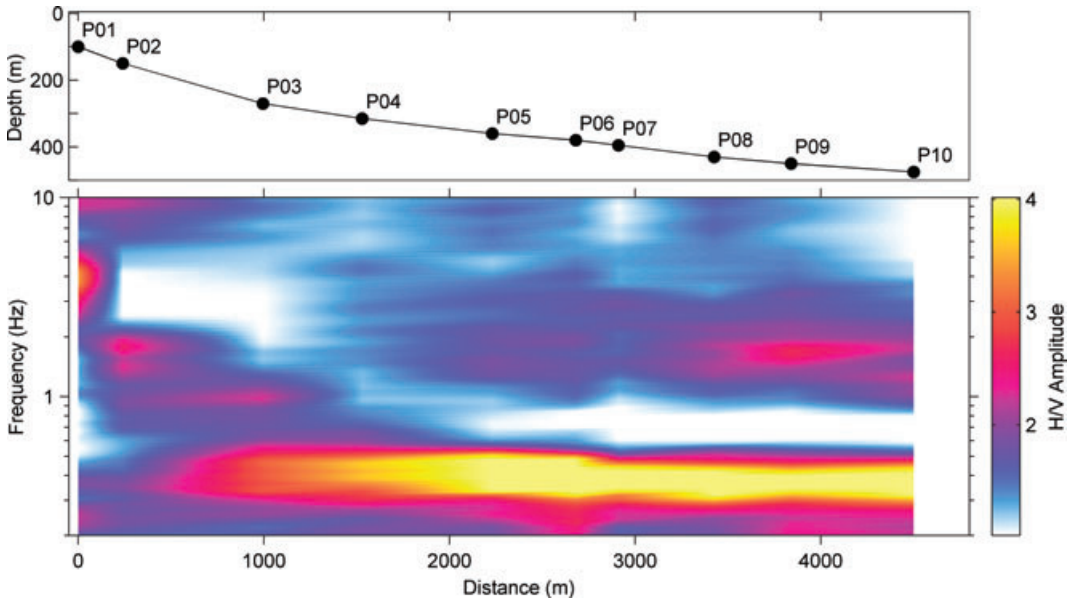

Figure 8. (top) Depth estimation of rock substratum (black circles) given by gravimetric study (Araneda *et al.* 2000) at points P01 to P10 of the *H/V* profile shown Fig. 6. (bottom) *H/V* spectral ratio amplitude as a function of distance along the profile.

from site to site. In the Santiago case, however, *H/V* curves exhibit a more complex pattern, without any prominent peak, or with several distinct bumps. One question immediately arises after this: is it possible to infer the site resonance frequencies from fuzzy *H/V* data?

5.1 Clear peaks

When the *H/V* peak is clear, then the site under study presents a large velocity contrast at some depth, and is very likely to amplify the ground motion (see for instance Konno & Ohmachi 1998; Bard & SESAME-Team 2005). In the case of Santiago, this fact is supported by Fourier amplitude spectra computed from strong ground motions stations by Cruz *et al.* (1993). These authors report amplification factors of about 2.6 on pumice sites and 4 on unconsolidated-soil sites. In addition, under those circumstances, the SESAME recommendations also claim that the amplification of ground motion occurs at the *H/V* peak frequency. We look for testing this former statement for the Santiago case study by comparing the *H/V* peak frequencies with fundamental frequency inferred from earthquake data. Horizontal-to-vertical spectral ratio method (Lermo & Chavez-Garcia 1993) was applied to earthquake data recorded at three strong ground motion stations operated by the University of Chile (CL2, PCQ and RCDM; Fig. 9). At each frequency, only data with signal-to-noise ratio higher than 3 was selected. Low to moderate magnitude (3.9–5.3) earthquakes were recorded from 2003 to 2006. Thus, the earthquake Fourier amplitude spectra may lack information at low frequencies. As a consequence, we consider only frequencies above 0.6 Hz to compare ambient noise *H/V* peak frequencies and fundamental frequency inferred from earthquake data.

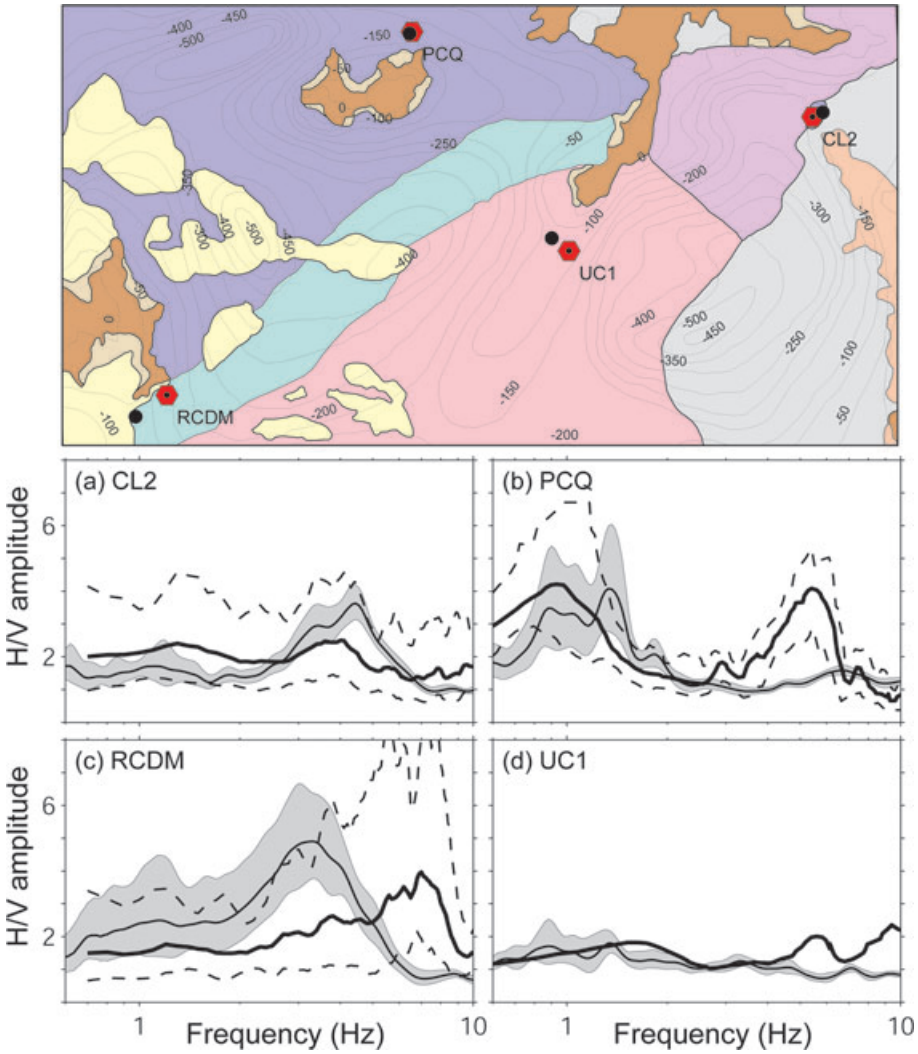

Figure 9. (top) Geological map (see legend Fig. 7) and location of the accelerometers stations (red hexagons) operated by the University of Chile (stations CL2, PCQ, RCDM) and the Catholic University of Chile (UC1) and nearby *H/V* data (black dots). (bottom) Earthquake horizontal-to-vertical spectral ratio computed at the strong ground motion stations (a) CL2, (b) PCQ, (c) RCDM, and (d) amplitude spectra ratio computed at UC1 (after Cruz *et al.* 1993). Black thick lines and dashed lines indicate the average spectral ratio and the associated standard deviation, respectively. At each station, *H/V* ratio (thin black line and greyed area) computed at the nearby ambient noise data are also shown.

The good agreement between the two former frequencies is depicted in Figs 9(a) and (b), outlining the robustness of the *H/V* method to provide the fundamental frequency in case of clear *H/V* peak, at least in Santiago. Fig. 9(c), however, illustrates well the limitation of the *H/V* method in case of broad band amplification of strong ground motion. The seismic amplification starts at the *H/V* peak frequency and remains large even though the *H/V* amplitude decreases. The *H/V* method provides thus the lower amplification frequency only, as already observed by Lebrun *et al.* (2001). The reason for the former limitation is not clear yet. It may be related to the horizontal polarization of Rayleigh waves, which is involved in the origin of the *H/V* peak (Konno & Ohmachi 1998; Bonnefoy-Claudet *et al.* 2006b). The influence of Love wave on the *H/V* ratio has been also pointed out by Arai & Tokimatsu (2000) and Bonnefoy-Claudet *et al.* (2008).

In the scientific literature dealing with site effects assessment and seismic microzonation, the usual practice is to plot the spatial distribution of site amplification frequencies as contour map. This representation, however, may become inappropriate in the case of Santiago because we have a low number of data (clear *H/V* peaks) non-equally distributed at the surface of the basin. We have then decided to depict the spatial location of *H/V* peak frequencies with respect to their frequency: 0.3–0.5 Hz, 0.501–1.2, 1.201–5 and 5.01–10 Hz. The intervals of frequency have been arbitrary chosen so that there is a roughly similar number of data for the first three intervals. *H/V* peak frequencies are displaying in Fig. 10, and we can make the following comments:

- 80 per cent of data with peak frequency between 0.3–0.5 Hz are located above the thickest parts of the basin, from 550 to 250 m, outlying the good correlation between low fundamental frequency and thick sediment deposits given by gravimetric study, at least to a first order.
- 75 per cent of data with peak frequency between 0.501–1.2 Hz are located above thinner sediment deposits, from 250 to 150 m, outlying once again the good correlation between fundamental frequency and sediment thickness.
- 25 per cent data with peak frequency between 1.201–5 Hz are located near basin edges and outcrops where the thickness of the sediment deposit ranges between 50 to 100 m, indicating once

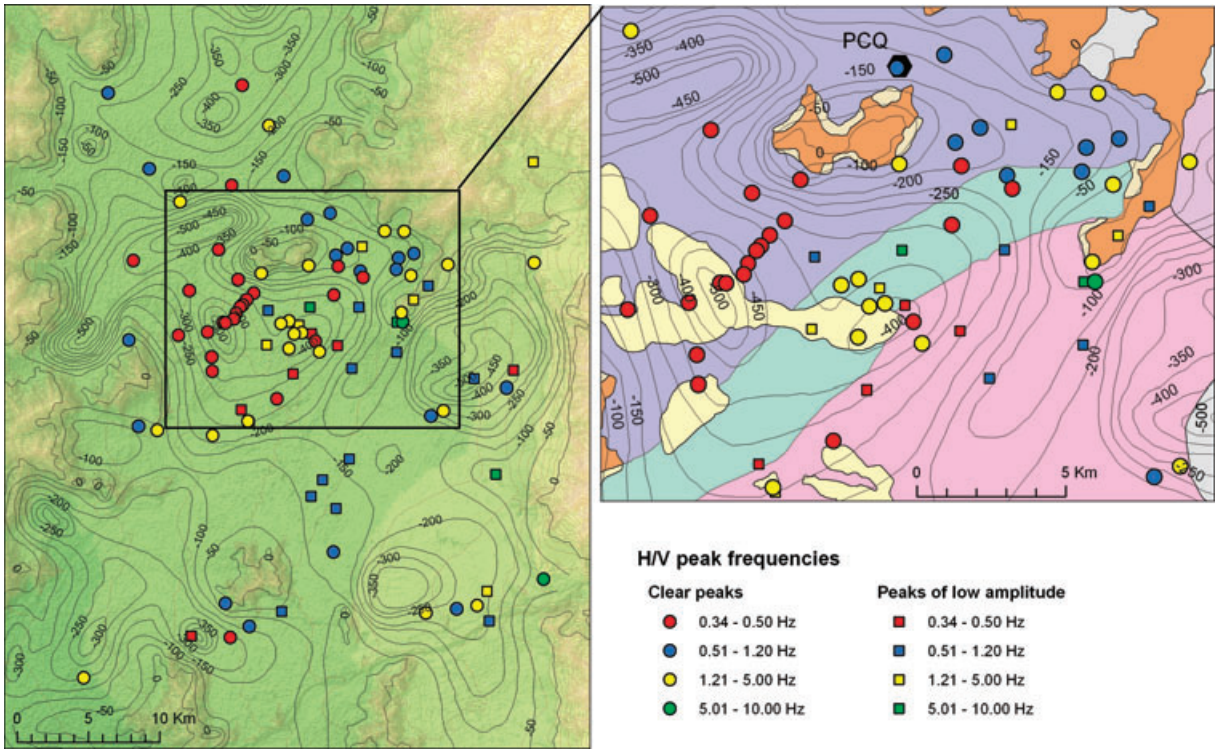

Figure 10. Spatial distribution of the *H/V* peaks according to their frequencies: (red) 0.3–0.5, (blue) 0.51–1.2, (yellow) 1.21–5 and (green) 5.1–10 Hz. Circles display frequencies for clear peaked *H/V* curves, whereas squares depict frequencies for peaks of low amplitude. The surface geology is shown in background, see Fig. 7 for legend. The location of the accelerometer station PCQ is shown in black hexagon.

more the correlation between fundamental frequency and sediment thickness. However, a large number of data (40 per cent) are located above deep depressions. These data cannot be related to the resonance of the deep sediment deposits (more than 250–400 m); they are more likely linked to the resonance of superficial deposits. Clear evidence can be found in the Pudahuel district where high frequency *H/V* peaks are distributed at the surface of the stiff pumice deposits.

- finally, data with peak frequency above 5.01 Hz are scattered at the surface of the basin, suggesting the presence of a topmost soft sedimentary layer (few metres thick).

Fig. 10 depicts thus the good agreement between the variations of the sediment thickness and the *H/V* peak frequency. For example, the PCQ site is characterized by alternating soft layers of silts and clays from surface to about 15 m depth; with an *S*-wave velocity at the surface around 150 m s^{-1}. Below, dense gravels, with an *S*-wave velocity estimated at 480 m s^{-1} (Table 1), reach the bedrock at a depth of about 100 m (Midorikawa *et al.* 1991; Toshinawa *et al.* 1996). The mean *S*-wave velocity (by means of average travel time) within the sediments is 360 m s^{-1}; and the use of the simple relation $f_0 = \beta/4h$ leads to a site resonance frequency of about 0.9 Hz. This value agrees with the expected amplification frequency at this site (inferred from microtremor and earthquake *H/V* data, see Fig. 9b), suggesting that when the *H/V* peak frequency is clear, the *H/V* method can be safely used as an alternative tool to classical geophysical exploration techniques for characterizing sediment infilling (typically sediment thickness if shear-wave velocity is known, see for instance Ibs-Von Seht & Wolhenberg 1999; Delgado *et al.* 2000; Parolai *et al.* 2002).

5.2 Flat curves and *H/V* peaks of low amplitude

Flat *H/V* curves and *H/V* peaks of low amplitude are both located at the surface of dense sediment formations: Mapocho and Santiago gravels. Such low amplitude *H/V* curves observed on no-rock site are a strong indication of stiff sediment underlain by bedrock and in such situation one may expect a rather small amplification in case of earthquake (Lachet & Bard 1994; Bard 1998; Konno & Ohmachi 1998; Bonnefoy-Claudet *et al.* 2008). In the case of Santiago, this assumption is supported by looking at Fourier amplitude spectra computed from strong ground motions by Cruz *et al.* (1993) in the dense gravel area. For instance, the low level of site amplification at UC1 accelerometer station (the amplitude ratio spectra lay between 1.2 and 1.5) is depicted in Fig. 9(d).

Following SESAME guidelines (Bard & SESAME-Team 2005), in the case of peaks of low amplitude the safest attitude is to refrain from deriving quantitative interpretations from the *H/V* curve. Although the SESAME recommendations set the threshold for the *H/V* peak amplitude at 2, other studies are more relaxed. Bard (1998) suggests that an unclear bump on the *H/V* curve, followed by a clear trough, may also be used for the estimation of the fundamental frequency. In this sense, Rodriguez & Midorikawa (2002) also argue that proscribe *H/V* estimations relying solely on the small spectral ratios criterion becomes inadequate. In the case of Santiago, the spatial distribution of peak frequency of *H/V* data of low amplitude, below 2 (colour filled squares in Fig. 10) agrees well with the location of clear peaked *H/V* frequency; at least as a first order. This suggests that when peaks of low amplitude are spread among clear peaked curves, it may be possible to use the peak frequency

as a proxy of site resonance frequency. However, one may keep in mind that further experiments should be performed before systematically deriving quantitative information from *H/V* peaks of low amplitude.

5.3 Broad peaks

Broad *H/V* peaks are very likely related to a complex wavefield due to significant 2-D or 3-D variations of the underground structure, see Section 4. The propagation of microtremor seismic waves may involve diffracted waves (body and surface waves) generated along slope and discontinuities. In such situation, the 1-D wave propagation properties are no longer reliable and the origin of *H/V* ratio cannot be simply explained by the propagation of waves in a 1-D medium.

For a practical use of *H/V* ratio, it can be difficult to pick the *H/V* peak frequencies in case of broad peaks (see for instance Fig. 5d). Picking *H/V* peak frequency in such cases may lead to bias the actual fundamental site frequency. Recent findings of numerical simulations show 1-D resonance frequency underestimated by *H/V* peak frequencies (up to 80 per cent) at sites with steep underground slopes (Guillier *et al.* 2006). Unfortunately, the earthquake data collection in Santiago is not suitable to quantitatively investigate the shift in resonance frequency inferred from microtremor and strong ground motion data. Although there is no evidence of large deviation on actual data, we strongly suggest not inferring fundamental frequency from unclear *H/V* peak without having earthquake data simultaneously.

6 DISCUSSION

The 1985 March 03 Valparaiso earthquake (M_s 7.8, 17 Km deep, 33.13°S–71.87°W), was destructive enough to damage a considerable number of houses in Santiago. The intensity data for the Valparaiso earthquake were estimated based on damages report of one storey adobe and one storey masonry houses (Astroza *et al.* 1993). The determination of the intensity degree (in MSK) is based on the statistical behaviour of damages reported in 288 sectors (of one square kilometre) of Santiago city and for (1) only one type of construction of adobe houses and (2) two types of construction of unreinforced masonry houses (Astroza & Monge 1991). In total, the number of damaged houses is 16 538 for adobe houses and 21 827 for un-reinforced masonry houses. The vulnerability might thus be statistically the same for all adobe houses and for all unreinforced masonry houses. Most of the observed damage was concentrated in areas with poor soils conditions located in the northwest of the city, especially in the fine-grained alluvial deposits (Quilicura, Renca and Cerro Navia districts), in the stiff pumices (Pudahuel and Lo Prado), and in the transition zone (Quinta Normal; Fig. 11). Local site effects due to geological conditions were thus first suspected to happen. However, some discrepancies are notable. For instance, a cluster of damage is also reported in consolidated sediment (gravels), in the southern of the city (Puente Alto district), whereas areas in unconsolidated sediment report less damage (Conchali and Huerchuraba districts; Fernandez Mariscal 2003). The surface geology cannot thus fully explain the distribution of damage. The hypothesis of lateral propagation, in addition to 1-D resonance effect, responsible for the site amplification of seismic ground motion in Santiago may be appropriate here. However, clear evidence of such effects has to be analysed in more details before drawing any conclusion.

The damage pattern in urban areas during an earthquake depends on the characteristics of the event and on the interaction between site response and vulnerability of the exposed structures. During the last 15 yr several efforts have been made to correlate damage with surface geology properties estimated from ambient noise measurements. Several papers present the comparison between the

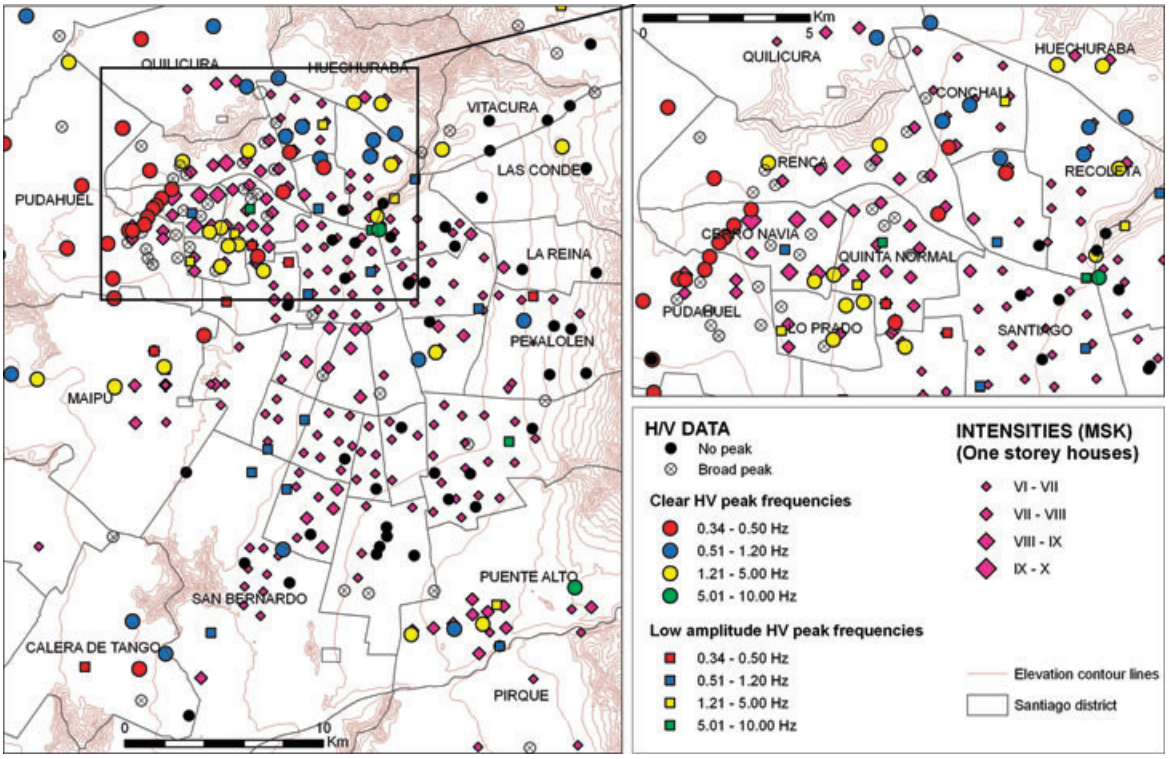

Figure 11. Comparison between the *H/V* data and the distribution of the felt intensities (MSK) in Santiago after the Valparaiso 1985 earthquake (Astroza & Monge 1987). Intensities were evaluated from one-storey—adobe and masonry—houses.

fundamental frequency and corresponding *H/V* amplitude level and damage distribution or macroseismic intensities after significant earthquakes (Theodoulidis *et al.* 2008 and references therein). Some of the studies indicate that the *H/V* results are correlated with the spatial distribution of damage, especially when damage variation is mostly controlled by near-surface geology. In the case of Santiago, during the 1985 Valparaiso earthquake, there was considerable damage to small-sized adobe structures, whereas the many high rise structures in the 10–20 storey range performed well with minor damage to finishes and non-structural features (Wyllie *et al.* 1986). Surprisingly, in the area of the highest intensities, the comparison between the *H/V* peak frequencies and damage on small-size houses reveals a discrepancy; although the *H/V* peak frequencies do not exceed 4—5 Hz, much damage was observed on small-size houses, which have an expected natural frequency higher than 5 Hz.

This discrepancy contradicts previous studies showing the correlation between the *H/V* data and the observed damage distribution. Here, the low frequency *H/V* peaks are linked to the deep velocity contrast at the basement and do not reflect the resonance of superficial soil layer. See, for instance, the comparison between microtremor and earthquake *H/V* curves observed at the PCQ accelerometer station (Fig. 9b): strong ground motion indicates site amplification at 5.75 Hz whereas the microtremor *H/V* ratio remains flat. Conversely, the origin of the discrepancy could be due to other processes than site effects that could have contributed to the damage and they are not captured by the noise measurements (vulnerability of structures, for instance). Beyond the possible explanations, this study shows the limits of the *H/V* technique in providing information that could be correlated to the damage distribution for the 1985 Valparaiso earthquake. The *H/V* method could not be used alone to assess a comprehensive seismic hazard zoning in urbanized area characterized by a large variety of buildings (from small-size houses to high buildings), such as Santiago de Chile.

7 CONCLUSIONS

Extensive ambient vibrations measurements (264 data) were performed in the basin of Santiago de Chile. We seek to verify the possibilities and limitations of the *H/V* spectral ratios technique (Nakamura 1989) to provide qualitative and quantitative information of site conditions. The interpretation of the *H/V* curve was carried out conformably to SESAME project consensus criteria (Bard & SESAME-Team 2005). According to these criteria, we first verified the curve reliability and then checked the clarity of the *H/V* peak. The application of the above criteria to the Santiago dataset results in 199 usable data showing 47 sites with flat *H/V* curves and 152 sites with peaked *H/V* curve.

The detailed analysis of microtremor data outlines three major patterns of *H/V* curves: (1) clear peaked curves, (2) flat *H/V* curves or curves showing peaks of low amplitude (namely below 2) and (3) curves exhibiting broad peak(s).

(1) In the case of clear *H/V* peaks, we show the reliability of the *H/V* method to provide a confident estimate of the fundamental resonance frequency. The *H/V* method can be safely used, in addition to geophysical and geotechnical data, to obtain either the velocity or the sediment thickness at the site of interest. It is thus a valuable tool for seismic risk assessment as long as it is used in combination with other methods.

(2) Conversely, the *H/V* curves having flat or low *H/V* amplitude are closely related to sites with lower impedance contrast, between deeper strata and upper sedimentary layer, with respect to the unconsolidated sediments (alluvial or ashes deposits). One should expect small amplification of strong ground motion during shaking at these sites. In addition, we show that, in the case of Santiago, *H/V* data exhibiting peaks of low amplitude (below 2) may also indicate the soil resonance frequency. These results suggest revising the quality criteria, stated by SESAME guidelines (Bard & SESAME-Team 2005), about the *H/V* peak amplitude threshold to assess the reliability of the *H/V* estimate. However, further work will be needed to answer this debate.

(3) Finally, we show, in agreement with previous studies (Uebayashi 2003), that broad *H/V* peaks might be an indication of the presence of a dipping underground interface between softer and harder layers at depth. It is likely that the underground structure of the site under study exhibits significant lateral variations, which could lead to significant 2-D or 3-D effects. Such broad peak *H/V* curves are indeed observed on many basin or valley edges, and we strongly suggest not inferring resonance frequency from such peaks without having earthquake data simultaneously.

With reference to site effect assessment in Santiago de Chile, the meticulous analysis of *H/V* data emphasizes three different seismic responses. The first is defined by stiff sediments (Mapocho and Santiago gravels) where no large site amplification is expected. The second is characterized by soft sediments (unconsolidated alluvial deposits and stiff pumice) where important ground motion amplification is very likely to occur. The third relies on the geometry of the stratification, in particular the bedrock inclination, where site amplification could be expected. Indeed, in such situation, the generation of edge-diffracted waves might be expected. These areas are mostly located near basin edges and next to underground slopes. However, further investigations are needed to quantify the seismic amplification in such cases.

For a practical use of *H/V* ratio and to ensure the reliability and the robustness of the *H/V* technique, we propose to carefully analyse the *H/V* data before mapping the soil resonance frequencies and doing microzonation in urban areas. The peculiar shape of the *H/V* curves is a reliable estimate of the underground site features. First, it provides a rough estimation of the strength of the impedance contrast: clear *H/V* peaks depict the presence of a strong underground contrast at depth, whereas unclear peaks of low amplitude—or flat curves—depict a low impedance contrast. Second, the broad width of the *H/V* peaks might be an indication of the presence of strong underground lateral variations. The results presented in this paper suggest using a dense spatial sampling of data and picking *H/V* frequencies only in areas showing a large proportion of clear *H/V* peaks.

The scrutiny of *H/V* data set recorded in Santiago allows us to keep only reliable data. This work outlines the need to carefully analyse the *H/V* data before picking the peak frequency and inferring quantitative estimation for microzonation purpose. The use of automatic (blind) zoning based on microtremor *H/V* ratios (see for instance Bragato *et al.* (2007)) may lead to severe errors in case of fuzzy *H/V* data like those observed in Santiago.

It is worth concluding by emphasizing that the *H/V* method alone is not enough to assess the seismic hazard in urbanized area especially when there is a large variety of buildings type: from small-size residential houses to high rise business buildings. A comprehensive seismic-risk evaluation could not be based only on *H/V* results. However, despite their limitations, the measurements of *H/V* microtremor spectral ratios are very informative for site effects estimating and remain a valuable input in urban seismic

microzonation, in the elaboration of a large earthquake scenario and in seismic hazard mitigation.

Finally, one should have special attention to the soil-sensor coupling, especially in urban areas where 'natural' ground surface is not always easily available. Records made on non-cemented pavement might produce large amplitude of *H/V* curve for frequencies below 1 Hz. In such cases, *H/V* curves have to be carefully analysed before inferring site effect estimates.

ACKNOWLEDGMENTS

We are very grateful to Chilean students who performed the extensive ambient vibrations measurements (José Lagos). We also thank Marc Wathelet for providing the software GEOPSY to compute *H/V* ratio. We also address our gratitude to two anonymous reviewers whose comments substantially improve our original manuscript. This research has been performed in the framework of joint collaboration between the Institute for Radioprotection and Nuclear Safety (Fontenay-aux-Roses, France) and the Department of Geophysics (University of Chile, Santiago, Chile). This work was supported by the Milenio project and ANR research program (France) under contract SUBCHILE).

REFERENCES

Arai, H. & Tokimatsu, K., 2000. Effects of Rayleigh and Love waves on microtremor H/V spectra, in *Proceedings of the 12th World Conference on Earthquake Engineering*, Auckland, New Zealand, January 30–February 4, paper 2232.

Araneda, M., Avendaño, M.S. & Merlo C., 2000. Modelo gravimetrico de la cuenca de Santiago, Etapa III final (In Spanish), in *Proceedings of the IX Congreso Geologico Chileno,* Puerto Varas, Chili, July 31–August 4, pp. 404–408, Sociedad Geologica de Chile.

Astroza, M. & Monge, J., 1987. Zonificacion sismica de la ciudad de Santiago, in *Proceedings of the XXIV Jornadas Sudamericanas de Ingeneria Estructural,*Vol. 5, Porto Alegre, Brasil, June 29–July 3, pp. 221–235, ANAIS, Porto Alegre, Brasil.

Astroza, M. & Monge, J., 1991. Seismic microzones in the city of Santiago. Relation damage-geological unit, in *Proceedings of the Fourth International Conference on Seismic Zonation,*Vol. 3, Stanford, CA, USA, August 25 –29, pp. 595–601, Earthquake Engineering Research Institute, Stanford, CA, USA.

Astroza, M., Monge, J. & Valera, J., 1993. *Intensidades del sismo del 3 de marzo 1985 en la region Metropolitana y el litoral central. Ingeneria sismica, el caso del sismo del 3 de marzo 1985* (In Spanish), Instituto Ingenieros de Chile, Ediciones Pedagogicas Chilenas S.A., Ediciones Dolmen, pp. 103–117.

Atakan, K., Duval, A.-M., Theodulidis, N., Guillier, B., Chatelain, J.-L., Bard, P.-Y. & SESAME-Team, 2004. The H/V spectral ratio technique: experimental conditions, data processing and empirical reliability assessment, in *Proceedings of the 13th World Conference on Earthquake Engineering,* Vancouver, Canada, 1–4 August, paper 2268.

Baize, S., Rebolledo, S., Lagos, J. & Rauld, R., 2006. A first-order model of the Santiago basin, in *Proceedings of the International Conference 1906 Valparaiso Earthquake Centennial,* Santiago de Chile, Chile, November 6–8.

Bard, P.-Y., 1998. Microtremor measurements: a tool for site effect estimation? in *Proceedings of the Second International Symposium on the Effects of Surface Geology on Seismic Motion,*Vol. 3, Yokohama, Japan, December 1–3, pp. 1251–1279, Balkema: Rotterdam, Yokohama, Japan.

Bard, P.-Y. & SESAME-Team, 2005. Guidelines for the implementation of the H/V spectral ratio technique on ambient vibrations–measurements, processing and interpretations, SESAME European research project EVG1-CT-2000–00026, deliverable D23.12, available at http://sesame-fp5.obs.ujf-grenoble.fr.

Barrientos, S., Vera, E., Alvarado, P. & Monfret, T., 2004. Crustal seismicity in central Chile, *J. South Am. Earth Sci.,* **16,** 759–768.

Bonnefoy-Claudet, S., Cornou, C., Bard, P.-Y., Cotton, F., Moczo, P., Kristek, J. & Fäh, D., 2006a. H/V ratio: a tool for site effects evaluation. Results from 1-D noise simulations, *Geophys. J. Int.,* **167,** 827–837.

Bonnefoy-Claudet, S., Cotton, F. & Bard, P.-Y., 2006b. The nature of noise wavefield and its applications for site effects studies. A literature review, *Earth.-Sci. Rev.,* **79,** 205–227.

Bonnefoy-Claudet, S., Köhler, A., Cornou, C., Wathelet, M. & Bard, P.-Y., 2008. Effects of Love waves on microtremor H/V ratio, *Bull. seism. Soc. Am.,* **98,** 288–300.

Bour, M., Fouissac, D., Dominique, P. & Martin, C., 1998. On the use of microtremor recordings in seismic microzonation, *Soil. Dyn. Earthq. Eng.,* **17,** 465–474.

Bragato, P., Laurenzano, G. & Barnaba, C., 2007. Automatic zonation of urban areas based on the similarity of H/V spectral ratios, *Bull. seism. Soc. Am.,* **97,** 1404–1412.

Bravo P.R., 1992. Estudio geofisico de los suelos de fundacion para une zonificacion sismica del area urbana de Santiago Norte (In Spanish), *PhD thesis*. University of Chile, Santiago de Chile, Chile.

Chatelain, J.-L., Guillier, B., Cara, F., Duval, A.-M., Atakan, K. & Bard, P.-Y., 2008. Evaluation of the influence of experimental conditions on H/V results from ambient noise recordings, *Bull. Earthq. Eng.,* **6,** 33–74.

Cornou, C., 2002. Traitement d'antenne et imagerie sismique dans l'agglomération grenobloise (Alpes françaises): implications pour les effets de site (In French), *PhD thesis*. University Joseph Fourier, Grenoble, France.

Cornou, C., Bard, P.-Y. & Dietrich, M., 2003. Contribution of dense array analysis to identification and quantification of basin-edge induced waves, part II: application to the Grenoble basin (French Alps), *Bull. seism. Soc. Am.,* **93,** 2624–2648.

Cruz, E., Ridell, R. & Midorikawa, S., 1993. A study of site amplification effects on ground motions in Santiago, Chile, *Tectonophysics,* **218,** 273–280.

DeMets, C., Gordon, R., Argus, D. & Stein, S., 1994. Effect of recent revisions to the geomagnetic time scale on estimates of current plate motions, *Geophys. Res. Lett.,* **21,** 2191–2194.

Delgado, J., Lopez Casado, C., Giner, J., Estevez, A., Cuenca, A. & Molina, S., 2000. Microtremor as a geophysical exploration tool: Application and limitations, *Pure appl. Geophys.,* **157,** 1445–1462.

Di Giulio, G., Cornou, C., Ohrnberger, M., Wathelet, M. & Rovelli, A., 2006. Deriving wavefield characteristics and shear-velocity profiles from two-dimensional small-aperture arrays analysis of ambient vibrations in a small-size alluvial basin, Colfiorito, Italy, *Bull. seism. Soc. Am.,* **96,** 1915–1933.

Duval, A.-M., Méneroud, J.-P., Vidal, S. & Singer, A., 1994. Relation between curves obtained from microtremor and site effects observed after Caracas 1967 earthquake, in *Proceedings of the 11th European Conference on Earthquake Engineering,* Paris, France, 6–11 September.

Falcon Moreno, E., Castillo Urrutia, O. & Valenzuela Muñoz, M., 1970. Hidrogeologia de la Cuenca de Santiago (In Spanish), Publication especial No3, Instituto de Investigaciones Geologicas, Santiago, Chile.

Fäh, D., 1997. Microzonation of the city of Basel, *J. Seism.,* **1,** 87–102.

Fernandez Marescal, J.C., 2003. *Respuesta sismica de la Cuenca de Santiago, region metropolitana de Santiago, Escala 1:100000, 1 mapa*. SERNAGEOMIN, carta geologica de Chile, Serie Geologia Ambiental, 1. ISSN:0717–7305.

Gardi, A., Lemoine, A., Madariaga, R. & Campos, J., 2006. Modeling of stress transfer in the Coquimbo region of Central Chile, *J. geophys. Res.,* **111,** B04307.

Guéguen, P., 1994. Microzonage de santiago du Chile (technique de Nakamura) (In French), *Master Thesis*. Joseph Fourier University, Grenoble, France.

Gueguen, P., Cornou, C., Garambois, S. & Banton, J., 2007. On the limitation of the H/V spectral ratio using seismic noise as an exploration tool: application to the Grenoble valley (France), a small apex ratio basin, *Pure appl. Geophys.,* **164,** 115–134.

Guillier, B., Cornou, C., Kristek, J., Moczo, P., Bonnefoy-Claudet, S., Bard, P.-Y. & Fäh, D., 2006. Simulation of seismic ambient vibrations: does the H/V provide quantitative information in 2D-3D structures? in *Proceedings of the Third International Symposium on the Effects of Surface Geology on Seismic Motion,* Grenoble, France, August 29–September 1, Paper 185.

Ibs-Von Seht, M. & Wohlenberg, J., 1999. Microtremor measurements used to map thickness of soft sediments, *Bull. seism. Soc. Am.,* **89,** 250–259.

Iriarte-Diaz, S., 2003. Impact of urban recharge on long-term management of Santiago Norte aquifer, Santiago–Chile, *Master thesis*. Waterloo University, Notario, Canada.

Kawase, H., 1996. The cause of the damage belt in Kobe:"the basin-edge effect", constructive interference of the direct S-wave with the basin-induced diffracted Rayleigh waves, *Seism. Res. Lett.,* **67,** 25–34.

Konno, K. & Ohmachi, T., 1998. Ground-motion characteristics estimated from spectral ratio between horizontal and vertical components of microtremor, *Bull. seism. Soc. Am.,* **88,** 228–241.

Lachet, C. & Bard, P.-Y., 1994. Numerical and theoretical investigations on the possibilities and limitations of Nakamura's technique, *J. Phys. Earth,* **42,** 377–397.

Lay, T. et al., 2005. The great Sumatra-Andamman earthquake of 26 december 2004, *Science,* **308,** 1127–1133.

Lebrun, B., Hatzfeld, D. & Bard, P.-Y., 2001. A site effect study in urban area: experimental results in Grenoble (France), *Pure appl. Geophys.,* **158,** 2543–2557.

Lermo, J. & Chavez-Garcia, F., 1993. Site effect evaluation using spectral ratios with only one station, *Bull. seism. Soc. Am.,* **83,** 1574–1594.

Lermo, J. & Chavez-Garcia, F., 1994. Are microtremors useful in site response evaluation?, *Bull. seism. Soc. Am.,* **84,** 1350–1364.

Midorikawa, S., Riddell, R. & Cruz, E., 1991. Strong-ground accelerograph array in Santiago, Chile, and preliminary evaluation of site effects, *Earthq. Eng. Struct. Dyn.,* **20,** 403–407.

Monge, J., 1986. *El sismo del 3 de marzo 1985, Chile* (In Spanish), 2nd edn, Acero Comercial, Santiago de Chile, Chile.

Morales-Jerez, F.R., 2002. Definicion de aquiferos en la Cuenca del Rio Maipo (In Spanish), *Master thesis*. University of Chile, Santiago de Chile, Chile.

Mucciarelli, M., Gallipoli, M., Di Giacomo, D., Di Nota, F. & Nino, E., 2005. The influence of wind on measurements of seismic noise, *Geophys. J. Int.,* **161,** 303–308.

Nakamura, Y., 1989. A method for dynamic characteristics estimation of subsurface using microtremor on the ground surface, *Q.R. Rail. Tech. Res. Inst.,* **30,** 25–30.

Nogoshi, M. & Igarashi, T., 1971. On the amplitude characteristics of microtremor, Part 2 (In Japanese with English abstract), *J. Seism. Soc. Japan,* **24,** 26–40.

Olsen, K.B. & Archuleta, R.J., 1996. Three dimensional simulation of earthquakes on the Los Angeles fault system, *Bull. seism. Soc. Am.,* **86,** 575–596.

Pardo, M., Comte, D. & Monfret, T., 2002. Seismotectonic and stress distribution in the central Chile subduction zone, *J. South Am. Earth Sci.,* **15,** 11–22.

Parolai, S., Bormann, P. & Milkreit, C., 2002. New relationships between Vs, thickness of sediments, and resonance frequency calculated by the H/V ratio seismic noise for the Cologne area (Germany), *Bull. seism. Soc. Am.,* **92,** 2521–2527.

Rodriguez, H.S. & Midorikawa, S., 2002. Applicability of the H/V spectral ratio of microtremors in assessing site effects on seismic motion, *Earthq. Eng. Struct. Dyn.,* **31,** 261–279.

Rovelli, A., Scognamiglio, L., Marra, F. & Caserta, A., 2001. Edge-diffracted 1-sec surface waves observed in a small-size intramountain basin (Colfiorito, Central Italy), *Bull. seism. Soc. Am.,* **91,** 1851–1866.

Theodoulidis, N., Cultrera, G., De Rubeis, V., Cara, F., Panou, A., Pagani, M. & Teves-Costa, P., 2008. Correlation between damage and ambient noise H/V spectral ratio: the SESAMEproject results, *Bull. Earthq. Eng.,* **6,** 109–140.

Toshinawa, T., Matsuoka, M. & Yamazaki, Y., 1996. Ground-motion characteristics in Santiago, Chile, obtained by microtremor observations, in *Proceedings of the 11th World Conference on Earthquake Engineering,* Acapulco, Mexico, 23–28 June, Paper 1764.

Uebayashi, H., 2003. Extrapolation of irregular subsurface structures using the horizontal-to-vertical ratio of long-period microtremors, *Bull. seism. Soc. Am.,* **93,** 570–582.

Uetake, T. & Kudo, K., 1998. The excitation of later arrivals in Ashigara valley during earthquakes occurring in east part of Yamanashi prefecture, in *Proceedings of the Second International Symposium on the Effects of Surface Geology on Seismic Motion,* pp. 427–434, Balkema: Rotterdam, Yokohama, Japan.

Valenzuela, G.B., 1978. Suelo de fundacion del gran Santiago (In Spanish with English abstract), *Instituto de Investigaciones Geologicas,* **33,** 1–27.

Wyllie, L. et al., 1986. The Chile earthquake of March 3, 1985, *Earthq. Spectra,* **2,** 293–371.

Woolery, E.W. & Street, R., 2002. 3D near-surface soil response from H/V ambient-noise ratios, *Soil. Dyn. Earthq. Eng.,* **22,** 865–876.

Yalcinkaya, E. & Alptekin, O., 2005. Contributions of basin-edge-induced surface waves to site effect in the Dinar bain, Southwestern Turkey, *Pure appl. Geophys.,* **162,** 931–950.